Activity-Stability Parameterization of Homogeneous Green Oxidation Catalysts

Arani Chanda,[a] Alexander D. Ryabov,[a] Sujit Mondal,[a] Larissa Alexandrova,[a, b] Anindya Ghosh,[a] Yelda Hangun-Balkir,[a] Colin P. Horwitz,[a] and Terrence J. Collins*[a]

Abstract: Small-molecule synthetic homogeneous-oxidation catalysts are normally poorly protected from self-destruction under operating conditions. Achieving design control over both activity and half-life is important not only in advancing the utility of oxidation catalysts, but also in minimizing hazards associated with their use and disposal. Iron(III)-TAML (tetraamido-macrocyclic ligand) oxidant catalysts rapidly activate H_2O_2 for numerous significant processes, exhibiting high and differing activity and varying half-lives depending upon the TAML design. A general approach is presented that allows for the simultaneous determination of the second-order rate constant for the oxidation of a targeted substrate by the active catalyst (k_{II}) and the rate constant for the intramolecular self-inactivation of the active catalyst (k_i). The approach is valid if the formation of the active catalyst from its resting state and the primary oxidizing agent, measured by the second-order rate constant k_I, is fast and the catalyst concentration is very low, such that bimolecular inactivation pathways can be neglected. If the oxidation process is monitored spectrophotometrically and is set up to be incomplete, the kinetic trace can be analyzed by using the equation $\ln\left(\ln\frac{A_t}{A_\infty}\right) =$ $\ln\left(\frac{k_{II}}{k_i}[Fe^{III}]_{tot}\right) - k_i t$, from which k_{II} and k_i can be determined. Here, A_t and A_∞ are absorbances at time t and at the end of reaction ($t = \infty$), respectively, and $[Fe^{III}]_{tot}$ is the total catalyst concentration. Several tools were applied to examine the validity of the approach by using a variety of different Fe^{III}-TAML catalysts, H_2O_2 and tBuOOH as oxidizing agents, and the dyes safranine O and orange II as target substrates. Learning how catalyst activities (k_{II}) and catalyst half-lives (k_i) can be controlled by ligand design is an important step in creating green catalysts that will not persist in the environment after they have achieved their purpose.

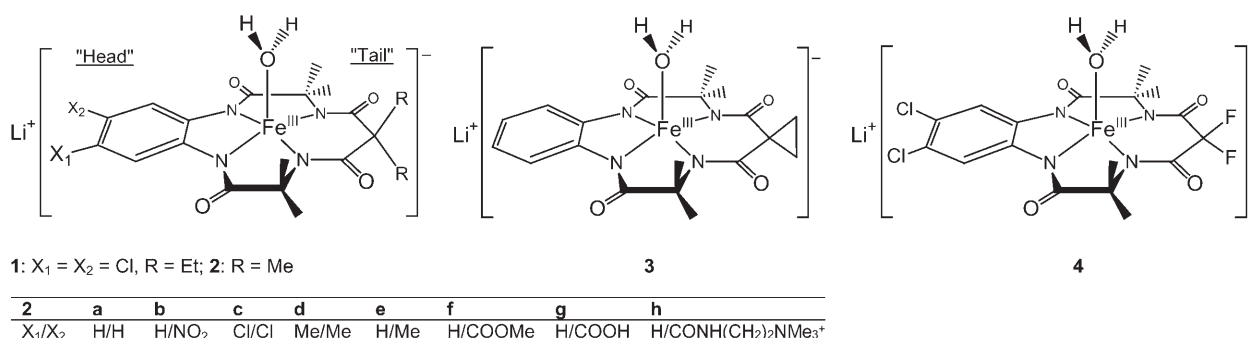**Keywords:** environmental chemistry · Fe-TAML · green chemistry · homogeneous catalysis · ligand design

Introduction

The central goal of green chemistry is to reduce or eliminate hazards from chemical products and processes.[1] Here we describe the temporal quantification of an approach for avoiding potential hazards associated with the release of residual active catalysts from oxidation processes. Catalysts are core enablers of innumerable chemical technologies. They generally improve process selectivity, energy intensity, operating time, capital costs, and overall economic and environmental features. Catalyst fate may be a significant factor in both the economic and environmental performances of any technology. Catalyst technologies can be categorized into three groups based upon the catalyst's fate. The first group comprises technologies in which the catalyst functions throughout most of its lifecycle in a reactor until it is removed for recovery or disposal. Here, the catalyst's fate can be most effectively controlled. The second group consists of technologies in which the catalyst is incorporated into the product. Here the catalyst follows the path of the product through its uses to its ultimate disposal—environmental and health impacts are possible at each step along the way. The third group encompasses technologies in which the catalyst, in spent and/or active form, is ejected directly into the environment as a component of an effluent stream. Here, as with the second group, there may also be significant health

[a] A. Chanda, Dr. A. D. Ryabov, Dr. S. Mondal, Dr. L. Alexandrova, A. Ghosh, Y. Hangun-Balkir, Dr. C. P. Horwitz, Prof. T. J. Collins
Department of Chemistry, Carnegie Mellon University
4400 Fifth Avenue, Pittsburgh, PA 15213 (USA)
Fax: (+1) 412-268-1061
E-mail: tc1u@andrew.cmu.edu

[b] Dr. L. Alexandrova
On leave from Instituto de Investigaciones en Materiales
UNAM, Circuito Exterior s/n, Ciudad Universitaria
Mexico, DF, 04510 (Mexico)

1: $X_1 = X_2 = Cl$, R = Et; **2**: R = Me   **3**   **4**

2	a	b	c	d	e	f	g	h
X_1/X_2	H/H	H/NO$_2$	Cl/Cl	Me/Me	H/Me	H/COOMe	H/COOH	H/CONH(CH$_2$)$_2$NMe$_3^+$

Scheme 1. Iron(III)-TAML catalysts of H_2O_2 used in this work.

and environmental issues. The subject catalysts of this present study, Fe^{III}-TAMLs (Scheme 1), belong to the third group.

A number of overt and latent hazards need to be considered whenever a catalyst is released into environmental media. Firstly, catalysts are often based upon metals that are unfamiliar or foreign to the biosphere. For this reason, they may be toxic or ecotoxic at the inception of the technology. However, for rare metals, toxicity is often poorly understood and any candid acknowledgement of scientific limitations would include the concession that unforeseen catalyst hazards could accompany commercial activity. Additionally, catalyst ligands or their degradation products could be sources of hazard. Secondly, catalysts that activate naturally occurring reagents present potential for hazard if they are ejected in functioning form into environmental media—their chemistry as opposed to their composition may be hazardous. This possibility must be considered especially for homogeneous catalysts that activate oxygen or its derivatives, peroxides, or superoxide. Fe^{III}-TAML catalysts fall into this reactivity category. They are powerful peroxidase mimics that, inter alia, offer benefits for effluent treatment in the pulp and paper[2–4] and textile industries.[5] At the least sophisticated level of process design, the catalysts and their degradation products would be components of the waste streams of these industries.

The Fe^{III}-TAML catalysts undergo a series of reactions (Scheme 2). Firstly, the catalysts interact with peroxide to produce the active catalyst (k_I). Then, not only do they oxidize substrates in a peroxidase-like fashion (k_{II}),[6–8] but they
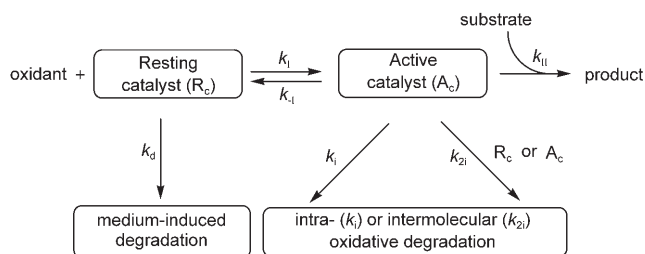
also decompose peroxide in a catalase-like manner.[8] The work presented here was conducted under conditions in which the catalase-like activity could be reasonably ignored.[8] In solution, the Fe^{III}-TAML catalyst can undergo medium-induced degradation (k_d), such as hydrolysis, however, this is pH-dependent and known to be insignificant at the pHs employed in this study.[9] Under operating conditions, Fe^{III}-TAML catalysts also undergo intramolecular (k_i) and intermolecular (k_{2i}) suicide inactivation. Any attempt to analyze quantitatively how design control over Fe^{III}-TAML catalyst half-lives can be used to optimize utility and obviate reactivity-derived latent hazards requires that the rate constants of each of these processes be determined for a series of catalysts and examined to gain insight into how the different elementary reactions influence each other.

For optimizing the green-process characteristics, the relationship between a Fe^{III}-TAML catalyst's half-life and its reactivity can be stated in terms of the underlying elementary reactions as follows. The Fe^{III}-TAML catalyst should decompose completely by the end of the process, but the half-life, as determined by k_i and/or k_{2i}, should not be significantly shorter than the time required for a very large number of catalytic turnovers, as determined by k_{II}. In this report, we describe a general approach for the simultaneous determination of the catalytic rate constants, k_{II}, and the intramolecular inactivation rate constants, k_i, for catalysts **1–4**. We relate these rate constants to the structural features of Fe^{III}-TAML catalysts and the composition of the reaction medium. We also evaluate the trends that provide the highest catalytic activity and stability of the oxidation catalysts **1–4**.

Results and Discussion

Preliminary observations: Kinetic measurements of the Fe^{III}-TAML-catalyzed oxidation of conventional dyes, such as pinacyanol chloride, safranine O, and orange II, by H_2O_2 revealed that oxidation does not follow monoexponential kinetics under pseudo-first-order conditions, that is, under at least ten-fold excess of H_2O_2 over all dyes used. Consequently, the initial-rate approach was applied to examine the peroxidase-like and catalase-like activities of the Fe^{III}-TAML catalysts.[8] The data shown in Figure 1 illustrate the
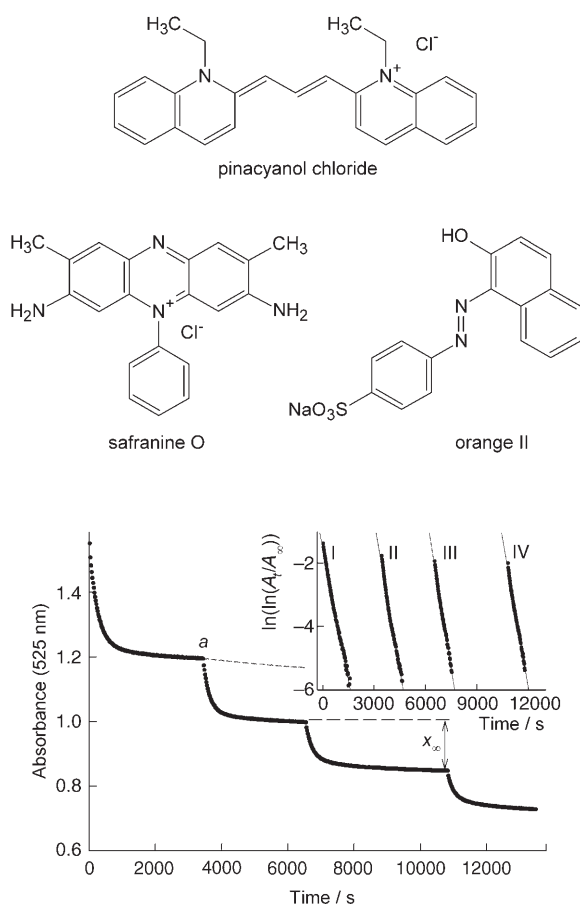

Scheme 2. Major catalytic steps and the steps leading to the inactivation of the resting state and the active form of an oxidation catalyst involved in a two-substrate process.

Figure 1. Kinetics of **2a**-catalyzed bleaching of safranine O (4.3×10^{-5} M) by H_2O_2 (0.012 M). Initial concentration of **2a** = 7.5×10^{-8} M; aliquots of the same amount of **2a** were added after complete inactivation of the catalyst, giving rise to the stepped dependence. The dashed line shows that addition of 0.012 M H_2O_2 does not resume the catalytic bleaching. Inset shows linearization of the data obtained after each addition of **2a** according to Equation (5). Conditions: pH 11, 25 °C.

nonexponential kinetics. The **2a**-catalyzed bleaching of safranine O was initiated by addition of an aliquot of H_2O_2. At low catalyst concentrations the bleaching does not go to completion, even if $[H_2O_2] \gg [\text{dye}]$.

Addition of the second aliquot of H_2O_2 at time a does not restart catalytic bleaching (Figure 1), suggesting deactivation of the catalyst. Accordingly, addition of a new aliquot of **2a** resumes the reaction. The bleaching of safranine O can be completed by successive additions of **2a** (Figure 1 shows incomplete bleaching). The robustness of safranine O toward oxidation by Fe^{III}-TAMLs and H_2O_2 makes it convenient for studying Fe^{III}-TAML catalyst half-lives.

General kinetic model for parameterization: A methodology for quantifying the catalytic performance based on Scheme 2 is required. The intermolecular inactivation will be assumed to be kinetically insignificant at this point, that is, $k_{2i} \approx 0$, because the majority of the dye-bleaching experiments were run at very low catalyst concentrations (10^{-6}–10^{-8} M). Therefore, second-order pathways should not play a

substantial role. The medium-induced hydrolytic degradation is known to be kinetically insignificant under the conditions employed herein. Iron(III)-TAML catalysts are subject to H$^+$-catalyzed demetalation, for which the pseudo-first-order rate constant is given by $k_{obs} = k_\alpha[\text{H}^+] + k_\gamma[\text{H}^+]^3$.[9] The demetalation becomes significant at pH ~ 4 for **2a**, a methyl-tailed TAML catalyst, but only at significantly lower pH for **4**, a fluorine-tailed TAML catalyst. The bleaching experiments reported here were performed in the pH range 10–12 and, therefore, k_d is negligible. There is an additional dihydrogenphosphate-dependent demetalation of **2a** at pH 5–7, which is also unimportant because its timescale is much longer than that of the dye bleaching that underlies the kinetic determinations—this demetalation process is not observed for the fluorine-tailed **4**.[10]

The stoichiometric mechanism of catalysis shown in Scheme 2 is based on kinetic investigations of the Fe^{III}-TAML-catalyzed oxidation of various electron donors by peroxides.[8] The rate constants k_I, k_{-I}, and k_{II} in Scheme 2 are effective, pH-dependent parameters, and the oxidant is an organic peroxide or H_2O_2. Under the steady-state assumption applied to active catalyst (A_c) and by using the mass-balance equation for the catalyst, $[\text{Fe}^{III}]_{tot} = [\text{Fe}^{III}] + [A_c]$, the rate of substrate oxidation by H_2O_2 is given by Equation (1):

$$-\frac{d[\text{substrate}]}{dt} = \frac{k_I k_{II}[\text{Fe}^{III}][\text{H}_2\text{O}_2][\text{substrate}]}{k_{-I} + k_I[\text{H}_2\text{O}_2] + k_{II}[\text{substrate}]} \tag{1}$$

A straightforward evaluation of the rate constants k_i and k_{II} is feasible if k_{-I} is negligible and the interaction between the Fe^{III}-TAML catalyst and H_2O_2 is significantly faster than the oxidation of the substrate itself, that is, if the relation $k_I[\text{H}_2\text{O}_2] > k_{II}[\text{substrate}]$ holds. This condition does not usually hold for low-molecular-weight catalysts of hydrogen peroxide, such as iron porphyrins.[11] In contrast to peroxidase enzymes,[12] the interaction of synthetic catalysts with H_2O_2 is usually the slowest step in the oxidation process. In general, this is also true for the Fe^{III}-TAML catalysts, although the second-order rate constants k_I are as high as 10^4 M^{-1} s^{-1} at pH of around 10, at which Fe^{III}-TAMLs display maximal activity[8] and the relation $k_I[\text{H}_2\text{O}_2] > k_{II}[\text{substrate}]$ can be secured by controlling concentrations. There are two ways of forcing the relation $k_I[\text{H}_2\text{O}_2] > k_{II}[\text{substrate}]$. The first approach accepts the use of dyes of moderate reactivity, employing high concentrations of H_2O_2, and selecting reaction conditions that ensure the highest-achievable k_I. As shown below, this can be attained with the dye orange II at pH ≈ 10.6. Alternatively, difficult-to-oxidize dyes with low values of k_{II} can be used. This opens a broader pH range for characterization of the operational stability of the Fe^{III}-TAML catalysts.

Safranine O belongs to the class of dyes that are difficult to oxidize by Fe^{III}-TAMLs. If the relation $k_I[\text{H}_2\text{O}_2] > k_{II}[\text{substrate}]$ holds, the initial rate (v) of its bleaching should be directly proportional to [safranine O] and independent of $[\text{H}_2\text{O}_2]$. The data shown in Figure 2 prove that
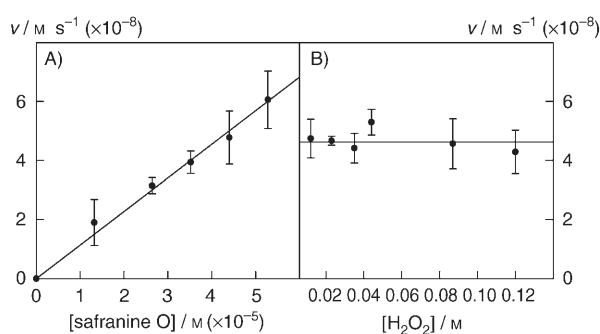
Figure 2. Initial rates (v) of **2a**-catalyzed (7.5×10^{-8} M) safranine O bleaching against A) safranine O concentration at $[H_2O_2] = 0.012$ M and B) H_2O_2 concentration at $[dye] = 4.3 \times 10^{-5}$ M. Conditions: pH 11, 25 °C.

this holds, therefore, safranine O is an ideal dye for the quantification of kinetic data, such as in Figure 1. The first- and zero-order dependencies in [safranine O] and $[H_2O_2]$, respectively, prove that k_{-I} is negligible compared to the $k_I[H_2O_2]$ term. Thus, Equation (1) can be simplified to Equation (2):[13]

$$-\frac{d[\text{substrate}]}{dt} = k_{II}[\text{substrate}][\text{Fe}^{III}] \qquad (2)$$

According to Scheme 2, the intramolecular inactivation of active forms of catalysts **1–4** is monoexponential. The corresponding rate constant is k_i. Therefore, the related differential equation for dye bleaching is given by Equation (3)

$$-\frac{d(D_t-x)}{dt} = k_{II}(D_t-x)([\text{Fe}^{III}]_{tot}e^{-k_i t}) \qquad (3)$$

in which D_t and $[\text{Fe}^{III}]_{tot}$ are total concentrations of the dye and a Fe^{III}-TAML catalyst, respectively, and x is the concentration of a bleached dye at time t. Integration of Equation (3) under the boundary conditions $x = x_\infty$ ($x_\infty =$ final concentration of bleached dye obtained with a single catalyst aliquot) if $t = \infty$ affords either Equation (4)

$$\ln\left[\ln\left(\frac{D_t-x}{D_t-x_\infty}\right)\right] = \ln\left(\frac{k_{II}}{k_i}[\text{Fe}^{III}]_{tot}\right) - k_i t \qquad (4)$$

or Equation (5)

$$\ln\left(\ln\frac{A_t}{A_\infty}\right) = \ln\left(\frac{k_{II}}{k_i}[\text{Fe}^{III}]_{tot}\right) - k_i t \qquad (5)$$

Equation (5) involves easy-to-measure absorbances A_t and A_∞ at time t and ∞, respectively, instead of concentrations as in Equation (4). Equation (5) suggests a simple procedure for analysis of data, such as in Figure 1. If the double logarithm of the ratio A_t/A_∞ is plotted against time, the slope of the straight line will be $-k_i$. The rate constant k_{II} can then be calculated from the intercept that equals $\ln(k_{II}[\text{Fe}^{III}]_{tot}/k_i)$. A linearization of the kinetic traces of Figure 1 in terms of Equation (5) is demonstrated in the

inset of Figure 1. All four steps in Figure 1 were analyzed. The values of k_i and k_{II} are summarized in Table 1—nearly identical rate constants k_i and k_{II} were calculated from each

Table 1. Rate constants k_i and k_{II} calculated from the data in Figure 1 by using Equation (5). Each pair of rate constants was obtained from a part of the curve after adding a new portion of **2a** to a solution of safranine O and H_2O_2 at pH 11 and 25 °C.

Run	$k_i \times 10^3$ [s^{-1}]	$k_{II} \times 10^4$ [M^{-1}s^{-1}]	
		from [Eq. (5)]	from initial rates[a]
1	3.1 ± 0.4	1.5 ± 0.4	1.3 ± 0.2
2	3.3 ± 0.3	1.4 ± 0.3	1.1 ± 0.1
3	3.3 ± 0.4	1.1 ± 0.1	1.1 ± 0.2
4	3.4 ± 0.3	1.1 ± 0.3	1.0 ± 0.2

[a] Calculated from the data in Figure 1 by using the relationship $k_{II} = v/[\textbf{2a}][\text{safranine O}]$ by analyzing initial rates (v) after adding a new portion of **2a**.

trace in Figure 1. The value of k_i indicates that the half-life of **2a** is 3.4 min under the operating conditions (25 °C, pH 11). The rate constant k_{II} is $\approx 10^4$ M^{-1}s^{-1}. The rate constants k_I, also evaluated in separate studies,[8] are of the same order of magnitude under such conditions. The bleaching reactions were performed at $[H_2O_2] \sim 0.01$ M and [safranine O] $\sim 5 \times 10^{-5}$ M, so that the relation $k_I[H_2O_2] \gg k_{II}[\text{substrate}]$ always holds and, therefore, the bleaching is zero-order in $[H_2O_2]$ and first-order in [safranine O]. An equation similar to Equation (5) was used by Pocalyoko et al. for determining the effectiveness of *N*-methyl-3,4-dihydroisoquinolinium *p*-toluenesulfonate towards oxidation of calmagite by peracetic acid.[14]

Model validation 1: Careful inspection of the data in Figure 1 indicates that the total amount of bleached dye obtained per aliquot (x_∞) of **2a** is not constant and gradually decreases after each new addition. This phenomenon is understood in terms of the general kinetic model proposed. The solution of differential Equation (3) by using the boundary condition $x = 0$ at $t = 0$ leads to Equation (6)

$$\ln\frac{A_0}{A_t} = \frac{k_{II}}{k_i}[\text{Fe}^{III}]_{tot}(1-e^{-k_i t}) \qquad (6)$$

in which A_0 and A_t are optical densities at times $t = 0$ and t, respectively. Because $A_t = A_0 - x$, $x \to x_\infty$ as $t \to \infty$. Substitution and rearrangement result in Equation (7):

$$x_\infty = A_0\left(1 - e^{-\frac{k_{II}}{k_i}[\text{Fe}^{III}]_{tot}}\right) \qquad (7)$$

Equation (7) implies that x_∞ should be directly proportional to the starting concentration of dye or to the absorbance A_0. The straight line passing through the origin in Figure 3 confirms the proposed model. Moreover, the predicted slope of this line is 0.25 ± 0.04, based on the values of the rate constants k_{II} and k_i from Table 1 and the concentration of **2a** (7.5×10^{-8} M). The slope determined from the experimental data is 0.24 ± 0.02, which agrees well with the calculated value.
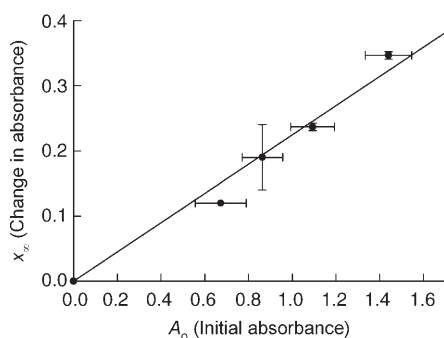
Figure 3. Dependence of the amount of bleached dye expressed as x_∞ on the total amount of dye expressed as A_0 for **2a**-catalyzed (7.5×10^{-8} M) bleaching of safranine O (initial concentration 4.3×10^{-5} M) by H_2O_2 (0.012 M) according to Equation (7) (see text for details). Conditions: 25 °C, pH 11.0.

Evaluation of catalytic performance of Fe^{III}-TAMLs: A qualitative difference in the efficacies for the bleaching of pinacyanol chloride by different Fe^{III}-TAML catalysts of H_2O_2 has been reported.[6] The **2**-type catalysts, for which R = Me, perform better than those for which R = Et (**1**), which was attributed to their longer half-lives. In these earlier studies, oxidative degradation pathways were determined at higher catalyst concentrations at which intermolecular suicide inactivation could not be ignored. It was established in nonaqueous solutions that the TAML ligand of **1** degrades primarily into an isolated and fully characterized metal-free hydantoin ring-containing product.[15] It is likely that **2** may share a related fate under higher Fe^{III}-TAML concentrations.[5] However, in the kinetic model explored here, in which lower concentrations are employed, it will be seen that different inactivation mechanisms might be operating.

Representative data obtained by using safranine O as the substrate dye are shown in Figure 4A. As anticipated, catalysts **1**, **2a**, **3**, and **4** display variable performance. The bleaching by **4** is both the deepest and the fastest. Equation (5) was applied to all kinetic traces in Figure 4A, affording the satisfactory straight lines shown in Figure 4B. The rate constants k_i and k_{II} summarized in Table 2 were
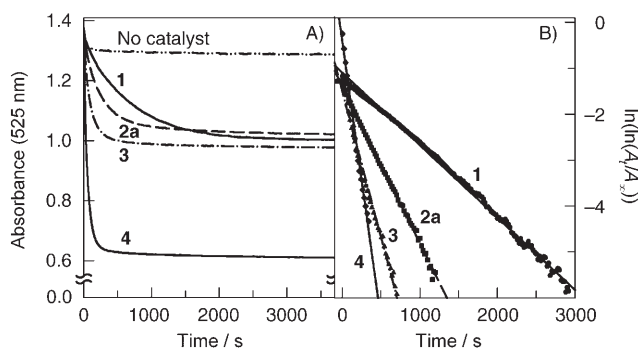
Table 2. Rate constants (k_i and k_{II}) calculated for different Fe^{III}-TAML catalysts at pH 11 from data, such as in Figure 4, by using Equation (5).

Catalyst	T [°C]	$k_i \times 10^3$ [s^{-1}]	$k_{II} \times 10^{-4}$ [M^{-1} s^{-1}]
1	13	0.44 ± 0.05	0.24 ± 0.03
	25	1.5 ± 0.1	0.7 ± 0.1
	42	5.7 ± 0.6	1.2 ± 0.1
	60	33 ± 3	3.6 ± 0.4
2a	13	1.9 ± 0.2	0.9 ± 0.1
	25	3.4 ± 0.3	1.1 ± 0.1
	42	5.2 ± 0.5	1.5 ± 0.2
	60	12 ± 1	3.1 ± 0.3
3	13	2.5 ± 0.3	0.99 ± 0.1
	25	6.2 ± 0.4	1.9 ± 0.2
	42	11 ± 1	3.6 ± 0.7
	60	18 ± 2	5.6 ± 0.6
4	13	4.8 ± 0.5	6.3 ± 0.6
	25	13 ± 1	10 ± 2
	42	20 ± 2	14 ± 1
	60	45 ± 2	23 ± 3

calculated from the slopes and intercepts, as described above. Similar experiments were performed at temperatures covering the 13–60 °C range. The inactivation (k_i) and bleaching (k_{II}) rate constants (Table 2) were used to calculate the corresponding enthalpies ($\Delta H^\ddagger$) and entropies ($\Delta S^\ddagger$) of activation by using the Eyring equation.[16] The numerical values are given in Table 3.

Table 3. Activation parameters $\Delta H^\ddagger$ [kJ mol^{-1}] and $\Delta S^\ddagger$ [J mol^{-1} K^{-1}] corresponding to the rate constants k_i and k_{II} for different Fe^{III}-TAML catalysts.[a]

Catalyst	$\Delta H_i^\ddagger$	$\Delta S_i^\ddagger$	$\Delta H_{II}^\ddagger$	$\Delta S_{II}^\ddagger$
1	67 ± 3	-73 ± 11	40 ± 5	-40 ± 15
2a	27 ± 3	-201 ± 10	18 ± 4	-108 ± 13
3	29 ± 4	-192 ± 14	26 ± 2	-76 ± 7
4	32 ± 5	-175 ± 15	18 ± 2	-89 ± 5

[a] $\Delta H^\ddagger$ and $\Delta S^\ddagger$ were measured at low H_2O_2 concentration (0.012 M); it is shown (see text) that they correspond to the $k_{i\alpha}$ pathway [Eq. (8)] because the $k_{i\beta}$ pathway is negligible under these conditions.

The rate constants in Table 2 reveal interesting trends: 1) The catalytic activity of Fe^{III}-TAMLs in bleaching safranine O (k_{II}) increases by more than ten-fold at 25 °C if the tail ethyl groups of **1** are replaced by fluorine atoms in **4**. The fluorine-tailed compound **4** is the most active. The rate constant k_{II} for **4** is 10^5 M^{-1} s^{-1} at 25 °C. The same level of reactivity is typical of horseradish peroxidase compound II toward anilines and phenols.[17,18] This emphasizes that Fe^{III}-TAMLs are really efficient synthetic low-molecular-weight peroxidase mimics. 2) The inactivation rate constants k_i also increase on progression from **1** to **4** and a similar ten-fold gap holds. Under the operating conditions ([H_2O_2] = 0.012 M, [safranine O] = 4.3×10^{-5} M, pH 11, and 25 °C), the half-lives, $\tau_{1/2}$, for catalysts **1** and **4** are 7.7 and 0.88 min, respectively. The difference in $\tau_{1/2}$ is less striking at 60 °C; 0.35 and 0.25 min, respectively.

Previously, we reported qualitative data showing the performance of the methyl-tailed catalyst **2c** to be better than

Figure 4. A) Kinetics of oxidation of safranine O (4.3×10^{-5} M) by H_2O_2 (0.012 M) by catalysts **1**, **2a**, **3**, and **4** (7.8×10^{-5} M). B) Linearization of the data according to Equation (5). Conditions: 25 °C, pH 11.0.

its ethyl counterpart **1** in the bleaching of pinacyanol chloride.[6] Although different inactivation processes are operating here, the quantitative kinetic data reported in this study also conform to the previous qualitative observations concerning comparative catalyst performances. Although the absolute values of rate constants k_i and k_{II} favor the **2c** catalyst only slightly (k_i: 1.1×10^{-3} vs. 1.5×10^{-3} s^{-1}; k_{II}: 1.1×10^4 vs. 0.7×10^4 M^{-1}s^{-1} for **2c** and **1**, respectively), the combined effects manifest in a considerable difference in the amount of safranine O that is bleached.

Our ongoing mechanistic studies of the Fe^{III}-TAML catalysts convincingly show that the introduction of fluorine atoms onto the tail dramatically changes the reactivity, allowing activation of H$_2$O$_2$ in acidic media (in addition to the basic range for these catalysts), and also producing significantly more-aggressive oxidizing systems. The modification of the "head", in contrast, induces considerably more-subtle changes in Fe^{III}-TAML-catalyst reactivity through aromatic-ring-mediated electronic effects, the structural features of the catalysts being otherwise the same.[8,9] We also examined how electron-donating or electron-withdrawing substituents at the aromatic ring affect the rate constants k_i and k_{II}.

Eight structurally similar, but electronically different, Fe^{III}-TAML catalysts **2**, for which R = Me, were investigated by applying Equation (5). The results, which are useful in practice, but are rather curious, are demonstrated in the linear free-energy relationship (LFER) of Figure 5. Al-
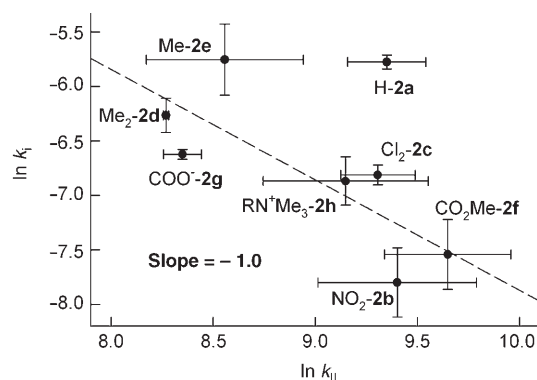

Figure 5. LFER between the rate constants k_{II} for bleaching safranine O and k_i for intramolecular inactivation in the series of "head"-substituted Fe^{III}-TAML catalysts with methyl tail groups. Conditions: [H$_2$O$_2$] = 0.012 M, 25°C, pH 11.0. See text for numbering. The data point for **2a** was ignored in the linear regression.

though the errors encountered in data collection require us to interpret with reservation, the trend in the variation of k_{II} and k_i seems to be clear. Electron-withdrawing substituents (NO$_2$, NMe$_3^+$, COOEt, Cl) increase the oxidizing power of the Fe^{III}-TAML catalysts with respect to safranine O (k_{II}), but retard the intramolecular inactivation (k_i). The most inactivation-resistant catalyst is the nitro-substituted Fe^{III}-TAML, **2b**, which is more stable than **2a** by a factor of six. This observation suggests that one of the vulnerable fragments of Fe^{III}-TAML catalysts is the aromatic component.

Presumably the active catalyst may destroy itself, initiated by oxidative damage at this group. Electron-withdrawing groups should protect the ligand system from this type of damage. Interestingly, the k_i value for **2a** is higher than that predicted by the other data in the LFER—if this value is neglected, the slope of the resulting straight line is -1.0 ± 0.3. This observation is unusual (a slope of $+1$ might be anticipated with more-reactive catalysts decomposing more rapidly) and it suggests a direct tool for tuning the catalytic activity and stability of Fe^{III}-TAML catalysts.

Enthalpies and entropies of activation: The activation parameters are summarized in Table 3. The values of $\Delta H_{II}^{\pm}$ are generally fairly low, 18–26 kJ mol^{-1}. Therefore, the rate of bleaching itself does not depend strongly on the temperature. The enthalpy of activation $\Delta H_{II}^{\pm}$ is somewhat higher for the ethyl-tailed complex **1**. The large and negative entropies of activation $\Delta S_{II}^{\pm}$ are typical of clean second-order processes.[16] The enthalpies of activation for the inactivation ($\Delta H_i^{\pm}$) are higher than $\Delta H_{II}^{\pm}$. Remarkably, as noted above, the $\Delta H_i^{\pm}$ of 67 kJ mol^{-1} for the ethyl-tailed **1** is significantly higher than the ~30 kJ mol^{-1} found for the other three catalysts. In practice, this means that **1** is comparatively and notably more vulnerable to the intramolecular inactivation at higher temperatures; the ratio $k_i(\mathbf{1})/k_i(\mathbf{4})$ is 0.09 at 13°C, but 0.73 at 60°C. The value of $\Delta S_i^{\pm}$ for **1** is significantly less negative than for other catalysts studied, indicating that the substitution of methyl for ethyl on the tail has a large influence on the intramolecular inactivation, although the meaning of this at the molecular level is still unclear. The large negative entropies of activation for the intramolecular inactivation of **2a**, **3**, and **4** indicate a highly ordered transition state.[16]

Effects of dye and H$_2$O$_2$ concentrations on k_i and k_{II}: The data in Figure 1 and Table 1 show that these rate constants are independent of the concentration of safranine O. The same values of k_i and k_{II} were obtained at different concentrations of the dye. In contrast, hydrogen peroxide affects the dye bleaching appreciably. As shown in Figure 6, more-extensive **2a**-catalyzed bleaching of safranine O is observed
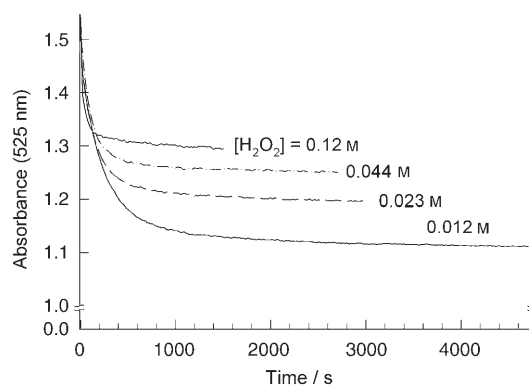

Figure 6. Bleaching of safranine O (4.3×10^{-5} M) catalyzed by **2a** (7.5×10^{-8} M) in the presence of different concentrations of hydrogen peroxide at pH 11 and 25°C.

at *lower* concentrations of H_2O_2. Only 19 % bleaching is achieved at $[H_2O_2] = 0.12\,\text{M}$. However, the conversion is 31 % at a ten-fold lower concentration of H_2O_2 (0.012 M). Similar behavior was reported previously for the oxidation of monochlorodimedon catalyzed by heme chloroperoxidase from *C. fumago*—monochlorodimedon is a substrate used for monitoring the activity of this enzyme.[19] Higher conversion was achieved at lower H_2O_2 concentrations. This was rationalized in terms of the H_2O_2-induced irreversible inactivation of chloroperoxidase. The rate constants for inactivation, k_i, exhibited Michaelis-type dependence on H_2O_2 concentration. Therefore, Equation (5) was applied to data, such as in Figure 6, for calculating k_i and k_{II} at differing $[H_2O_2]$. The data for the **2a** and **2b** catalysts are shown in Figure 7. The bleaching rate constants k_{II} are virtually insensitive to $[H_2O_2]$ in the range of 0.012–0.12 M. This supports the general mechanism suggested for Fe^{III}-TAML activation of H_2O_2, because the reactivity of the active intermediate should not depend on the H_2O_2 concentration.
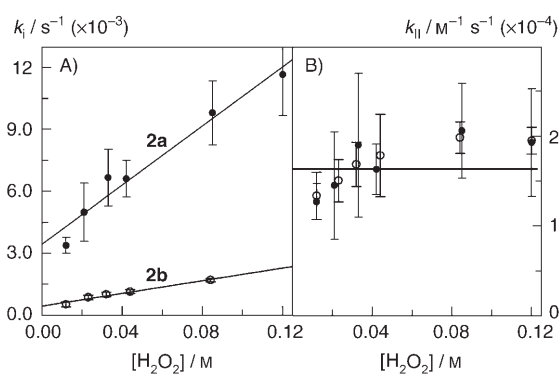

Figure 7. Effect of hydrogen peroxide concentration on the rate constants k_i (A) and k_{II} (B) for the **2a**- and **2b**-catalyzed bleaching of safranine O. Conditions: pH 11, 25 °C.

The inactivation rate constants k_i for **2a** and **2b** increase linearly as the H_2O_2 concentration increases, with a positive intercept. This suggests two pathways for the inactivation process, one zero-order and the other first-order in $[H_2O_2]$ (Eq. (8)):

$$k_i = k_{i\alpha} + k_{i\beta}[H_2O_2] \tag{8}$$

The form of Equation (8) guides one to keep $[H_2O_2]$ at the lowest possible level because, in addition to the catalase-like activity displayed by Fe^{III}-TAML catalysts at high $[H_2O_2]$ (resulting in waste of H_2O_2),[8] hydrogen peroxide is an inactivator of the Fe^{III}-TAML catalysts. The calculated rate coefficients $k_{i\alpha}$ and $k_{i\beta}$ for **2a,b** are summarized in Table 4. The H_2O_2-independent rate constant $k_{i\alpha}$ is associated with a suicide intramolecular inactivation pathway of the active catalysts. Notably, the value of $k_{i\alpha}$ is almost six times lower for the NO_2-ring-substituted catalyst **2b** than for its unsubstituted counterpart **2a**. As noted above for the composite k_i, this is a significant observation because variation

Table 4. Inactivation rate constants $k_{i\alpha}$ and $k_{i\beta}$ obtained in the course of bleaching of safranine O ($4.3 \times 10^{-5}\,\text{M}$) by using hydrogen peroxide as an oxidant at pH 11 and 25 °C.

Catalyst	$k_{i\alpha} \times 10^3\,[\text{s}^{-1}]$	$k_{i\beta}\,[\text{M}^{-1}\,\text{s}^{-1}]$
2a	3.2 ± 0.6	0.10 ± 0.01
2b	0.49 ± 0.03	0.014 ± 0.001

in the electronic properties of the head component of the catalysts appears to be a simple tool for their protection from the intramolecular inactivation. The $k_{i\beta}$ pathway, which is by a factor of ten more-pronounced for **2a** than for **2b**, should involve an external attack of hydrogen peroxide at the active catalyst. We consider there to be insufficient information available from the current data set to allow for further mechanistic interpretation of this newly recognized inactivation process.

Effect of pH on k_i and k_{II}: The influence of pH on the rate constants k_i and k_{II} was investigated employing **2a** in the pH range 10–12, at which the rate constant k_I is the highest,[8] so that the condition $k_I[H_2O_2] > k_{II}[\text{substrate}]$ holds most securely. The data obtained are shown in Figure 8, from which
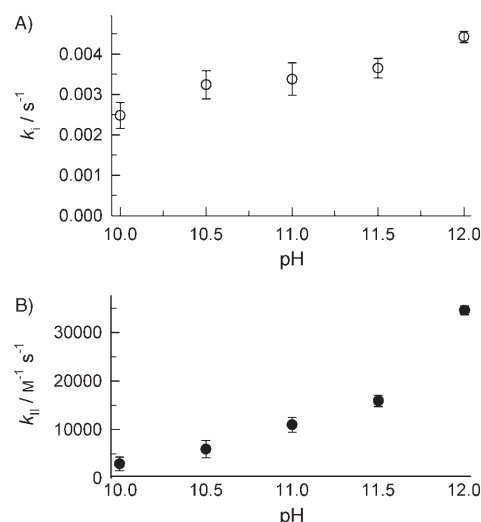

Figure 8. Effect of pH on the rate constants k_i (A) and k_{II} (B) for the **2a**-catalyzed bleaching of safranine O at 25 °C.

it can be construed that the dependence of k_i on pH is weak (Figure 8A), whereas k_{II} shows some increase as pH increases (Figure 8B).

Model validation 2: Orange II is an easier-to-bleach dye than safranine O. Studies of the kinetics of its bleaching by H_2O_2 and organic peroxides in the presence of **2a** indicate that the process follows Equation (1), that is, Michaelis kinetics are obeyed in [orange II] and [peroxide].[8] This implies that the required relation $k_I[H_2O_2] > k_{II}[\text{substrate}]$ is more difficult to achieve for orange II. However, it is possible to attain the required relation at pH ∼10–11 and high

peroxide and low orange II concentrations. Under such conditions the rate of bleaching is essentially independent of $[H_2O_2]$ and proportional to [orange II].[8] Therefore, Equation (5) was applied to the data obtained for the catalysts **2a** and **4**. The data for the bleaching of orange II were linearized in terms of Equation (5) and satisfactory straight lines were observed for both catalysts. The calculated rate constants k_i and k_{II} are summarized in Table 5 and the data for

Table 5. Rate constants (k_i and k_{II}) obtained for orange II and safranine O at 25 °C and $[H_2O_2] = 0.012$ M by using Equation (5). Orange II: pH 10.6, $[dye] = 7.2 \times 10^{-5}$ M, $[Fe^{III}] = 1.8 \times 10^{-8}$ M. Safranine O: pH 10.5, $[dye] = 4.3 \times 10^{-5}$ M, $[Fe^{III}] = 7.8 \times 10^{-8}$ M.

Rate constant	Catalyst	Orange II	Safranine O
$k_i \times 10^3 [s^{-1}]$	**2a**	4.2 ± 0.8	3.2 ± 0.4
	4	12 ± 2	10 ± 1
$k_{II} \times 10^{-4} [M^{-1} s^{-1}]$	**2a**	10.1 ± 0.4	0.6 ± 0.1
	4	31.1 ± 0.4	8.5 ± 1.8

safranine O is included for comparison. The inactivation rate constants k_i obtained by using different dyes under the same conditions are similar. The rate constants k_{II} are noticeably lower for safranine O than for orange II, as expected for the more-difficult-to-oxidize dye.

The kinetic methods employed for Fe^{III}-TAML/H_2O_2 reactions are also applicable to other oxidizing agents. The kinetic data obtained for **4**-catalyzed bleaching of safranine O by *tert*-butyl peroxide are summarized in Table 6. The rate

Table 6. Rate constants (k_i and k_{II}) obtained for safranine O (4.3×10^{-5} M) by using *tert*-butyl peroxide as an oxidant and catalyst **4** at pH 11 and 25 °C.

Peroxide used	Concentration [M]	$k_i \times 10^3 [s^{-1}]$	$k_{II} \times 10^{-4} [M^{-1} s^{-1}]$
*t*BuOOH	0.20	3 ± 1	1.4 ± 0.1
*t*BuOOH	0.17	3 ± 1	1.4 ± 0.1
H_2O_2	0.012	3.3 ± 0.5	1.0 ± 0.3

constant k_I for *t*BuOOH is more than ten times lower than for H_2O_2.[8] Provided the active intermediate is the same in both cases, similar values of k_i and k_{II} should be obtained, even when the concentration of *t*BuOOH is approximately a factor of ten greater than that of H_2O_2. As in the previous example, there is acceptable agreement. The information in Tables 5 and 6 implies that the nature of the dye and the oxidizing agent do not affect the rate constants for intramolecular inactivation, k_i. Therefore, the strategy developed and justified in this work appears to be "substrate independent" and can be applied, provided the relationship $k_I[ROOH] > k_{II}[substrate]$ holds.

Model validation 3: Equation (6) can be rearranged to a form [Eq. (9)] that describes the relative conversion of substrate, that is, A_t/A_0, as a function of time. Equation (9) provides a convenient means for simulating the catalyst performance by using the current model:

$$\frac{A_t}{A_0} = \exp\left\{ \frac{k_{II}}{k_i} [Fe^{III}]_{tot} (1 - e^{-k_i t}) \right\}^{-1} \qquad (9)$$

Thus, quantitative predictions can be compared with the experimental data. Equation (9) also destroys any illusion that Fe^{III}-TAML-catalyzed bleaching is always incomplete, as in Figures 1, 4 A, and 6. The "regime of incompleteness " was intentionally set up in this work as a tool for the evaluation of k_i. Figure 9 demonstrates different regimes of bleach-
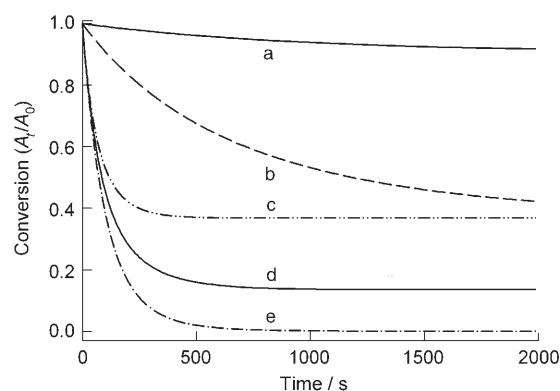
Figure 9. Simulated bleaching of a hypothetical dye by using Equation (9) at different concentrations of Fe^{III}-TAML catalyst. a) $[Fe^{III}] = 1 \times 10^{-8}$ M, $k_i = 1 \times 10^{-3}$ s^{-1}, $k_{II} = 1 \times 10^4$ M^{-1} s^{-1}; b) $[Fe^{III}] = 10 \times 10^{-8}$ M, $k_i = 1 \times 10^{-3}$ s^{-1}, $k_{II} = 1 \times 10^4$ M^{-1} s^{-1}; c) $[Fe^{III}] = 100 \times 10^{-8}$ M, $k_i = 10 \times 10^{-3}$ s^{-1}, $k_{II} = 1 \times 10^4$ M^{-1} s^{-1}; d) $[Fe^{III}] = 100 \times 10^{-8}$ M, $k_i = 5 \times 10^{-3}$ s^{-1}, $k_{II} = 1 \times 10^4$ M^{-1} s^{-1}; e) $[Fe^{III}] = 100 \times 10^{-8}$ M, $k_i = 1 \times 10^{-3}$ s^{-1}, $k_{II} = 1 \times 10^4$ M^{-1} s^{-1}.

ing that were calculated by using Equation (9). The bleaching is complete as the catalyst concentration reaches 10^{-6} M and $k_i \leq 10^{-3}$ s^{-1} (Figure 9e). At lower concentrations of Fe^{III}-TAML, the bleaching is slower and incomplete within the same time frame (Figure 9a,b). The bleaching becomes incomplete at higher catalyst concentrations ($[Fe^{III}] \geq 10^{-6}$ M) as k_i starts to rise (Figure 9c,d). Naturally, the degree of dye bleaching decreases as k_i increases.

Finally, additional support for the mechanistic concepts developed here would be provided by a good match between the experimental and predicted kinetic data calculated by using the obtained values of k_i and k_{II} at known concentrations of Fe^{III}-TAML catalysts. Provided the corresponding concentration regime is chosen, the calculated and measured absorbance-versus-time plots should be similar. Such a comparison is shown in Figure 10, in which the dynamics of **2a**-catalyzed bleaching of safranine O by hydrogen peroxide performed at different **2a** concentrations is plotted together with the calculated traces. There is excellent agreement between two experimental and calculated curves. This comparison proves that quantitative bleaching of the dye is in fact achieved simply by increasing the **2a** concentration. However, even after the increase, the concentration is very low, specifically, 10^{-6} M when the difficult-to-oxidize safranine O is bleached. Equation (5) was derived by putting rather severe limitations on the rate constants k_I and k_{II} in Scheme 2. If the relation $k_I[H_2O_2] > k_{II}[substrate]$
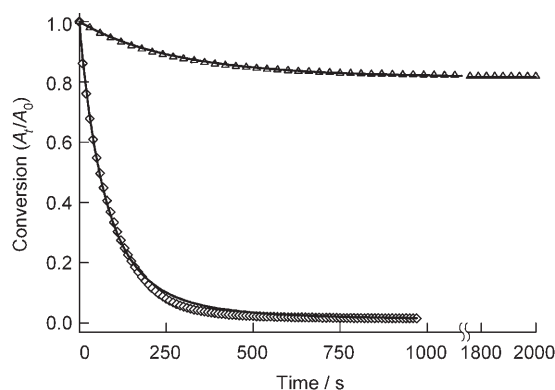
Figure 10. Normalized experimental and simulated bleaching of safranine O (4.3×10^{-5} M) by H_2O_2 (0.012 M) catalyzed by **2a** at pH 11 and 25 °C. △: [**2a**] $= 7.5 \times 10^{-8}$ M, $k_i = 3.3 \times 10^{-3}$ s^{-1}, $k_{II} = 0.9 \times 10^4$ M^{-1} s^{-1}. ◇: [**2a**] $= 1.0 \times 10^{-6}$ M, $k_i = 3.3 \times 10^{-3}$ s^{-1}, $k_{II} = 1.3 \times 10^4$ M^{-1} s^{-1}. The simulations, shown as solid lines, were made as in Figure 9 by using the rate constants from Table 1.

holds, there is an excellent coincidence between the experimental and simulated data. The approach described and justified herein is principally applicable to any two-substrate catalytic system, provided the activation of the catalyst is faster than a target chemical reaction.

In conclusion, green catalytic oxidation technologies are fully capable of supporting sustainable chemical products and processes. Fe^{III}-TAML catalysts begin to meet this promise in ways that are important for environmental integrity.[5,20,21] The results of this work increase their attractiveness for use in technologies that send effluent streams to environmental media, as there is now a clear scenario of how the activity of the catalysts affects their half-lives. This allows process conditions to be set to ensure that no live Fe^{III}-TAML catalyst remains at the point of exit of the effluent stream from the plant. A substantial gain in reactivity is brought about by fluorination of the tail component of Fe^{III}-TAMLs, however, this is accompanied by a drop in the half-lives of these more-reactive catalysts. Suicide inactivation is most efficiently retarded by introducing electron-withdrawing groups at the aromatic ring in the head part of Fe^{III}-TAMLs. Thus, knowing the rate constants k_i and k_{II} provides a shortcut for developing green oxidation technologies for which one can ensure the catalysts will be inactivated within the plant after they have performed their function.

Work is ongoing to quantify the relative importance of intermolecular pathways of Fe^{III}-TAML-catalyst inactivation, and this should also be significant in eventual process-optimization procedures. A further development of the approach described here involves solving the most general case without putting limitations on the ratio of rate constants k_I and k_{II}. This is important for cases in which significantly higher catalyst concentrations are used and in which the bimolecular suicidal-oxidative inactivation of Fe^{III}-TAML catalysts is driven by the rate constant k_{2i} (Scheme 2), to the point that it cannot be neglected in the modeling. An example of this is the killing of spores.[22]

Experimental Section

Materials and methods: Safranine O was purchased from Aldrich (>95% purity) and was used as received. Orange II (Aldrich) was purified by passing it through a column filled with SMT Bulk-C18 (Separation Methods Technologies, Newark) with a water/methanol mixture (9:1) as eluent. Hydrogen peroxide was purchased from Fluka and was standardized daily as described elsewhere.[23] All reagents, components of the buffer solutions, and solvents were of at least ACS reagent grade (Aldrich, Aldrich Sure-Seal, Fisher, Acros) and were used as received or were purified in an appropriate manner.[24] Fe^{III}-TAML **1** was prepared as described previously[15] and all other Fe^{III}-TAMLs **2–4** were synthesized according to procedures described either in patents[25] or elsewhere.[26,27] Spectrophotometric measurements were performed by using a Hewlett–Packard Diode Array spectrophotometer (model 8453) equipped with a thermostated cell holder and an automatic eight-cell positioner. Temperature was controlled by using a Thermo digital temperature controller RTE17 within an accuracy of ±1 °C. Both quartz and appropriate plastic cuvettes of the path length 1.0 cm were used to investigate spectral properties and for kinetic studies.

Spectral measurements: Kinetic measurements were performed at pH 10–12 in 0.01 M phosphate buffer by using HPLC-grade water. A stock solution of safranine O (31 mg in 10 mL, 8.8 mM) was prepared in water (HPLC grade) and was then transferred into the phosphate buffer to afford the required concentration of solution. Calibrated micropipettes were used for transferring solutions. Stock solutions of H_2O_2 were prepared from 30% H_2O_2 and were standardized by measuring the absorbance at 230 nm ($\varepsilon = 72.8$ M^{-1} cm^{-1}).[23] Fresh stock solutions (7.2 M) of *tert*-butyl hydroperoxide were used as prepared. Stock solutions of all Fe^{III}-TAML catalysts used in this study were prepared in water.

Kinetic studies: The kinetics of safranine O oxidation were analyzed by monitoring an absorbance decrease at 525 nm by using the pH-independent (pH 10–12) extinction coefficient of 3.3×10^4 M^{-1} cm^{-1}. The temperature was varied from 13 to 60 °C. The extinction coefficient of orange II was determined to be 1.2×10^4 M^{-1} cm^{-1} at pH 10–11. A typical kinetic run was performed as follows. Phosphate buffer (2 mL) was added to a thermostated cuvette. Appropriate amounts of stock solutions of safranine O and **1–4** were then added consecutively. The reaction was initiated by the addition of an aliquot of the stock solution of H_2O_2. The rates were calculated from the measured changes in absorbance over time by using the extinction coefficient for the dyes reported above.

Data analysis: Calculations of rate constants were performed by using Equations (5) and (6). All fits (both linear and nonlinear) were obtained by using a minimum r^2 value of 0.92. All rates reported are the mean values of at least three determinations. Simulations, nonlinear fitting of data, and all data analysis were performed by using the Sigma Plot 2001 package (Version 7.0).

[1] P. T. Anastas, J. C. Warner, *Green Chemistry: Theory and Practice*, Oxford University Press, Oxford, New York, Tokyo, **1998**.

[2] T. J. Collins, N. L. Fattaleh, L. D. Vuocolo, C. P. Horwitz, J. A. Hall, L. J. Wright, I. D. Suckling, R. W. Allison, T. J. Fullerton, *Pulping Conf., Montreal, Oct. 25–29*, **1998**, *Vol. 3*, 1291.

[3] T. J. Collins, C. P. Horwitz, *TAPPI Pulping Conf., Orlando, Oct. 31– Nov. 4*, **1999**, *Vol. 2*, 703.

[4] T. J. Collins, C. P. Horwitz (Carnegie Mellon University, USA), WO99/58634; [*PCT Int. Appl.* **1999**, 65].

[5] T. J. Collins, *Acc. Chem. Res.* **2002**, *35*, 782.

[6] C. P. Horwitz, D. R. Fooksman, L. D. Vuocolo, S. W. Gordon-Wylie, N. J. Cox, T. J. Collins, *J. Am. Chem. Soc.* **1998**, *120*, 4867.

[7] S. Sen Gupta, M. Stadler, C. A. Noser, A. Ghosh, B. Steinhoff, D. Lenoir, C. P. Horwitz, K.-W. Schramm, T. J. Collins, *Science* **2002**, *296*, 326.

[8] A. Ghosh, D. A. Mitchell, A. D. Ryabov, D. L. Popescu, T. J. Collins, unpublished results.

[9] A. Ghosh, A. D. Ryabov, S. M. Mayer, D. C. Horner, D. E. Prasuhn, Jr., S. Sen Gupta, L. Vuocolo, C. Culver, M. P. Hendrich, C. E. F. Rickard, R. E. Norman, C. P. Horwitz, T. J. Collins, *J. Am. Chem. Soc.* **2003**, *125*, 12378.

[10] V. Polshin, A. Ghosh, A. D. Ryabov, D. L. Popescu, C. P. Horwitz, A. Chanda, J. Henry, Y. Li, T. J. Collins, unpublished results.

[11] M. F. Zipplies, W. A. Lee, T. C. Bruice, *J. Am. Chem. Soc.* **1986**, *108*, 4433.

[12] H. B. Dunford, *Heme Peroxidases*, Wiley-VCH, Weinheim, **1999**.

[13] In a more general case, if the catalytic activity (active catalyst + $H_2O_2 \rightarrow Fe^{III}$-TAML + O_2 (k_{III})) is not ignored, the substrate consumption is given by $-d\ln[\text{substrate}]/dt = k_I k_{II}[Fe^{III}]/(k_I + k_{III})$. The rate constant k_{III} is lower than k_I under the conditions used and, therefore, Equation (2) is true.

[14] D. J. Pocalyko, J. L. Coope, A. J. Carchi, L. Boen, S. A. Madison, *J. Chem. Soc. Perkin Trans. 2* **1997**, 117. In this study, it was shown that the rate constant for the formation of the active species, oxaziridine, is approximately one third the rate for the oxidation of calmagite. This means that the application of Equation (5) is not always justified because the relation $k_I[\text{oxidant}] > k_{II}[\text{substrate}]$ may not hold. Therefore, erroneous conclusions could be made.

[15] M. J. Bartos, S. W. Gordon-Wylie, B. G. Fox, L. J. Wright, S. T. Weintraub, K. E. Kauffmann, E. Münck, K. L. Kostka, E. S. Uffelman, C. E. F. Rickard, K. R. Noon, T. J. Collins, *Coord. Chem. Rev.* **1998**, *174*, 361.

[16] J. H. Espenson, *Chemical Kinetics and Reaction Mechanisms*, 2nd ed., McGraw-Hill, New York, **1995**.

[17] D. Job, H. B. Dunford, *Eur. J. Biochem.* **1976**, *66*, 607.

[18] M. P. J. Van Deurzen, F. Van Rantwijk, R. A. Sheldon, *Tetrahedron* **1997**, *53*, 13183.

[19] A. N. Shevelkova, A. D. Ryabov, *Biochem. Mol. Biol. Int.* **1996**, *39*, 665.

[20] A. Ghosh, S. S. Gupta, M. J. Bartos, Y. Hangun, L. d. D. Vuocolo, B. A. Steinhoff, C. A. Noser, D. Horner, S. Mayer, K. Inderhees, C. P. Horwitz, J. Spatz, A. D. Ryabov, S. Mondal, T. J. Collins, *Pure Appl. Chem.* **2001**, *73*, 113.

[21] Y. Hangun, L. Alexandrova, S. Khetan, C. Horwitz, A. Cugini, D. D. Link, B. Howard, T. J. Collins, *Prepr. Pap.–Am. Chem. Soc. Div. Petr. Chem.* **2002**, *47*, 42.

[22] D. Banerjee, A. L. Markley, A. Ghosh, P. B. Berget, E. J. Minkley, S. K. Khetan, T. J. Collins, *Angew. Chem.* **2006**, *118*, 4078; *Angew. Chem. Int. Ed.* **2006**, *45*, 3974.

[23] P. George, *Biochem. J.* **1953**, *54*, 267.

[24] D. D. Perrin, W. L. F. Armarego, *Purification of Laboratory Chemicals*, 3rd ed., Pergamon Press, Oxford, **1988**.

[25] Key syntheses: http://www.chem.cmu.edu/groups/collins/awardpatpub/patents/index.html.

[26] Y. Hangun, PhD Thesis, Carnegie Mellon University (Pittsburgh, PA), **2002**.

[27] A. Ghosh, PhD Thesis, Carnegie Mellon University (Pittsburgh, PA), **2004**.